

LANDSAT TM band combinations for crop discrimination

Sherry Chou Chen, Getulio Teixeira Batista & Antonio Tebaldi Tardin

Departamento de Sensoriamento Remoto, Instituto de Pesquisas Espaciais (INPE), São José dos Campos, SP, Brasil

ABSTRACT: LANDSAT Thematic mapper provides not only more spectral bands but also improved spatial resolutions in the visible and infrared wavelengths as compared to the MSS data. However, problems are encountered by analysts in working with the increased number of wavelength bands. In order to learn how to analyze TM data for agriculture studies, LANDSAT data of a 15x15km area in Paraná State, Brazil, were acquired on Jan. 19, 1985. The predominant crops in the study area were soybeans, corn and sugarcane. To choose the best combination of three TM bands, which represents most information of the agricultural scene the entropy criterion was used. Once the triplet bands were chosen, the color of green, red and blue were associated to them according to the magnitudes of their variances to form the color composite. Interpretability of these color images were evaluated visually. For digital analyses the criterion of Jeffreys-Matusita distance was applied to verify the best band combination if 2,3,4 or 5 TM bands were used. A classification algorithm based on the maximum likelihood decision rule was then employed to classify the study area using the designated TM bands. Classification performances were compared pixel-by-pixel on alphanumeric printouts, the computer time consumed, the classification matrix and the upper bounds of the probability of error. After these analyses, the TM bands which should be used for an effective digital analysis of this agricultural scene were decided.

RESUMÉ: Le LANDSAT TM fournit davantage de bandes spectrales et une plus grande résolution spatiale que le MSS. Cependant, il existe des problèmes qui apparaissent lors de l'utilisation des sept bandes spectrales. Pour tester les données TM dans les applications agricoles, on a utilisé des données TM LANDSAT dans un carré de 15x15km dans l'État du Paraná (Brésil) durant le passage du LANDSAT, le 19 janvier 1985. Les principales cultures de la région étudiées étaient: soja maïs et canne à sucre. Pour choisir la meilleure combinaison des trois bandes TM qui comportent le plus d'informations intéressantes, on a utilisé le critère de l'entropie. Après le choix des trois bandes, les couleurs verte, rouge et bleue ont été associées à ces bandes selon les grandeurs de leur variance pour former une composition colorée. Les résultats de l'interprétation visuelle des images produites ont été comparés. Pour vérifier les meilleurs combinaisons de bandes pour la classification par ordinateur, on a utilisé le critère de la distance de Jeffreys-Matusita. Ensuite, on a utilisé un algorithme de classification qui utilise les meilleures combinaisons choisies pour 3,4 ou 5 bandes du TM. Des analyses ont été faites avec quatre types différents de présentation des résultats: a) les sorties alphanumériques; b) les matrices de classification; c) les limites supérieures de la probabilité d'erreur, et d) le temps d'ordinateur utilisé. D'après ces comparaisons la meilleure combinaison de bandes TM pour la classification des cultures a été déterminée.

1. INTRODUCTION

Since 1982 a new sensor, called the Thematic Mapper (TM), was mounted on the Land Observation Satellite (LANDSAT) together with the Multispectral Scanner System (MSS). The TM sensor provides data from seven better selected spectral regions. There are three bands from the visible, one from the near infrared (NIR), two from the middle infrared and one from the thermal infrared spectrum region. The reflected energy from the Earth surface is encoded into 8 bits per band, with an improved spatial resolution of 30m instead of the 6 bits data and 80m resolution provided by MSS. In short, the TM sensor has considerably better spectral, spatial, and radiometric resolution than the MSS system; consequently a superior data quality and a much larger data volume are obtained. This new sensor design was mainly for vegetation discrimination considering the characteristic spectral response of vegetation of the selected TM bands (Solomonson et al. 1980). Thus, TM data are expected to improve crop identification and area estimation accuracy in Paraná State, where the problem of strip fields is presented. However, one of the problem encountered in the analysis of TM data is to decide how to handle this huge data quantity efficiently. Experiences of the passed decade

demonstrated that for MSS data bands 4,5 and 7 are used to form false color composite, and for digital analysis, normally all four bands are employed, even though information contents of the two visible bands (band 4 and 5) or infrared bands (band 6 and 7) are intercorrelated. Now, for the seven TM bands, questions arise about which three bands should be used for color image production, and how to reduce the dimensionality of TM data for digital analysis in order to achieve cost-effective results considering the crop identification and area estimation accuracy and computer time consumed. The knowledge of how to produce color image using TM data for visual interpretation is especially important for developing countries, where the lacking of computer facility and properly trained analyzer are limitations for the implementation of digital analysis at local government agencies or research institutes. On the other hand, in many application areas, information contents can only be extracted by digital analysis. Thus, there is an urgent need for exploiting how to handle and analyze TM data both visually and digitally.

In this study TM band combinations for visual and digital analyses in an agricultural scene were investigated and the best band combination for crop discrimination was selected. Note that band 6 was not included in this study due to its low spatial resolution (120 m).

2. EXPERIMENTAL METHODS

Thematic Mapper digital data with path row annotation 223/76 were acquired on Jan. 19, 1985. Within this area, a segment, of 512x512 pixels, which locates on the margin of the Ivaí river and about 50 km south-west of Maringá, Paraná State, was selected for investigation. This segment was chosen not only due to its representativeness for the crops in the region, but also the cooperation provided by an agrobusiness company, where ground information such as crop type and variety, planting/harvesting dates, crop conditions, field practice, yield etc were available. On the date of imaging, predominant cover types in this subscene were soybeans, sugarcane, corn and gallery forest. Pasture and a small amount of reforestation and bare soil (i.e. plowed fields) were also presented. Soybeans were at the flowering stage, corn plantations were entering senescence, while sugarcane fields of various varieties were at different phenological stages and percentages of ground cover depending whether the field under consideration was planting or ratoon crop. Information contents of this segment was extracted from CCTs and stored on disk file for subsequent analyses. Based on the field information, 25 samples varying from 36 to 200 pixels, were chosen for the above cited cover types, and located on the image monitor of an interactive image analysis system in INPE. These sampled areas were used for band combination study and served later as training areas for supervised digital analysis.

2.1 Triplet band selection for color image composition

For color composition, a subset of 3 bands should be selected from the available TM bands and for this purpose we used the criterion of entropy. The technique of principle component analysis was not included because the color image resulted from the first three eigenvectors is scene dependent and the unknown color-surface relationships make the understanding of the physical meaning difficult. Any three TM bands form a three-dimensional feature space and the associated variance-covariance matrix defined an ellipsoid within the space. According to the entropy criterion, the triplet with the ellipsoid of the maximum volume should be chosen (Young and Calvert, 1984). The advantage of this criterion over other feature selection methods, based on the maximum total variance, is discouraging the inclusion of highly correlated bands in the selection. Theoretically, the maximum ellipsoid volume represents the maximum variation in tonality, thus it should be a proper criterion in band combination selection for color image production. In this study the entropy with and without a priori of normal distribution were both tested. Once the band triplet was chosen, the color assignment was made as suggested in Sheffield's study (1985): green, which is most sensitive to human eyes, is assigned to the band with the highest variance, red to the band of the second largest variance, and blue to the band of the smallest variance. The program implemented in our image analysis system gives the first six-band triplets, the prime colors were then assigned, slides were taken from the image monitor and visual evaluations were made on these slides for their interpretabilities.

2.2 Band selection for digital analysis

The best TM band combination for digital analysis should take into account the accuracy of the classification results and the computer time consumed. The discrimination function, "Jeffereys-Matusita distance" or the J-M distance, was used as the criterion for band combination. In multiclass classification problem we can choose the band

combination, which maximizes the mean J-M distance between two classes or that maximizes the minimum J-M distance. In this study both criteria were applied to select the best band combination if 2,3, 4 or 5 TM bands were used for digital analysis. Plotting the separabilities of the best 2,3,4 and 5 bands the optimal band combination was chosen. For classification, training statistics of the 25 samples were used to characterize the spectral responses of the cover types considered. These training statistics were then utilized to classify the whole area using a maximum likelihood decision rule of the image analysis system. Comparisons were made on: (1) alphanumeric print-outs (2) the classification matrix, (3) the computer time consumed, and (4) the upper bound of the probability of error by the J-M criterion. After these comparisons the best band combination for crop discrimination was selected.

3. RESULTS AND DISCUSSION

3.1 TM color image composite

Table 1 shows the basic statistics and coefficients of correlation for the six TM bands investigated. As expected, intercorrelations were found among visible bands, between bands 4 and 5 and between 5 and 7 for this highly vegetated area. The NIR band 4 has the highest variance and a wider spread of grey level indicating more information content than the other bands. Decreasing variances are observed from NIR to middle IR and then to the visible bands. The ranked first six band triplets by the entropy criterion, with and without the Gaussian priori, are listed in table 2. Independent to whether the priori was used or not, band 4 was the most important TM band for color compositing. The second band included in the triplet was band 5 and the last was a visible band or band 7. Once the band triplet was decided color coding was assigned according to the amplitudes of their variances; in our case green to the NIR band, red to middle-IR band and blue to the visible band. If both middle-IR bands were included in the combination, then red was assigned to band 5 and blue to band 7. Visual comparisons of slides taken from the image monitor for the selected color composites showed that when bands 4 and 5 were included in the band triplet together with any one of the visible bands or band 7, color appearances of vegetations were similar. Thus, we could not claim preference over any one of the combinations. Comparing the conventional false color composite (FCC); assigning blue to band 2, green to band 3 and red to band 4, to any of the ranked combinations no significant improvement in visual crop discrimination was noted. Under this condition the conventional FCC is favoured over the entropy selections because no additional training of photointerpreter on the color-surface relations is required. This conclusion, drawn from the 512x 512 pixels subscene, may be too local-specific. Acquisition of FCCs for the quadrant using conventional and the first ranked band combination will be requested for a further investigation.

3.2 Band selection for digital analysis

The ranked first six band combination, when 2,3,4 or 5 bands were used in digital analysis, are shown in table 3. Plotting the separabilities of the best combinations (Fig.1) we note that the statistical structure for crop discrimination had three or four dimensionalities. These results are in agreement with that obtained in previous studies by Townshend (1984) and Anuta et al. (1984). No matter whether the criterion of Max. J-M mean or Max. J-M min. was used, the best three- and four-band combinations, which should be included in digital analysis, were the same; they were bands 2-4-5 and

Table 1 -

	1
2	0.94
3	0.70
4	-0.07
5	0.22
7	0.30
\bar{x}	67.81
σ^2	10.12

*n = 512x512

Table 2 -

Rank	Entropy	Gaussian
	B*	
1	2	3
2	3	4
3	1	5
4	7	6
5	2	7
6	7	1

* Colors assigned
B = Blue

2-4-5-7 re
both combi
based on p
average or
upper bound
error was
three-band
(Table 4).
showed tha
soybeans,
time consu
this 512x5
than the f
difference
frame clas
another ad
considerat
three-band
example, f
compactabl
analysis 2
that for
bands 2,4
analysis.

4. CONCLUSIONS

LANDSAT TM
to select
compositio
conclusion
- Accord
5 and one
should be
However, n
discrimina
observed c
criterion,
2,3, and 4
color-surf
photointer

Table 1 - Correlation Matrix for LANDSAT-5 Thematic Mapper Subscene

	1	2	3	4	5	7
2	0.94					
3	0.70	0.74				
4	-0.07	-0.23	-0.50			
5	0.22	0.10	-0.22	0.75		
7	0.30	0.31	0.08	0.21	0.63	
\bar{x}	67.81	30.61	27.12	115.30	84.48	19.91
σ^2	10.12	21.60	76.23	1082.08	604.26	86.10

*n = 512x512 pixels

Table 2 - Ranked Results for the selection of Band Triplet to form color composite

Rank	Entropy Gaussian		with assumption	Entropy Gaussian		Without assumption
	B*	G	R	B	G	R
1	2	4	5	7	4	5
2	3	4	5	1	4	5
3	1	4	5	3	4	5
4	7	4	5	2	4	5
5	2	4	7	1	4	7
6	7	4	3	3	4	7

* Colors are assigned according to variances.

B = Blue G = Green R = Red

2-4-5-7 respectively. Classification performances of both combinations for the training areas were similar based on percentages of correct classification, average omission and commission error. The maximum upper bound of the probability of classification error was 9% for corn and sugarcane using the three-band and 7% for the four-band combination (Table 4). Comparison of alphanumeric printouts showed that no significant difference was found for soybeans, sugarcane and corn fields. The computer time consumed using the three-band combination for this 512x512 pixels area was five seconds shorter than the four-band's. This means a eleven-minute difference in computer processing time for a full frame classification which may not be crucial, but another advantage that has to be taken into consideration is the smaller data storage volume if three-bands are used in digital analysis. For example, for a quadrant scene only one CCT (computer compactable tape) is needed, while for four-band analysis 2 CCTs are required. Thus, we concluded that for crop discrimination of the study area TM bands 2,4 and 5 should be used in digital analysis.

4. CONCLUSIONS

LANDSAT TM data of an agricultural area were studied to select the best band combinations for color composition and digital analysis. The following conclusions are found:

- According to the entropy criterion band 4, band 5 and one band from either the visible or band 7 should be used as the triplet for color composition. However, no apparent improvement in visual discrimination of agricultural cover types was observed on the FCC, formed using the entropy criterion, comparing to the conventional FCC (bands 2,3, and 4). Thus, considering the well-established color-surface relations, which is known by most photointerpreters, the conventional FCC is selected

Table 3 - Ranked Results for Discrimination Using 2,3,4 or 5 Bands.

RANK	MAX. J-M _{mean}			
	2 Bands	3 Bands	4 Bands	5 Bands
1	4,5	2,4,5	2,4,5,7	2,3,4,5,7
2	2,4	3,4,5	2,3,4,7	1,2,4,5,7
3	3,4	2,4,7	1,2,4,5	1,2,3,4,5
4	4,7	1,4,5	3,4,5,7	1,3,4,5,7
5	3,5	3,4,7	2,3,4,7	1,2,3,4,7
6	2,5	2,3,4	1,3,4,5	1,2,3,5,7

RANK	MAX. J-M _{min.}			
	2 Bands	3 Bands	4 Bands	5 Bands
1	2,4	2,4,5	2,4,5,7	2,3,4,5,7
2	4,7	2,4,7	2,3,4,5	1,2,4,5,7
3	3,5	3,4,5	1,2,4,5	1,2,3,4,5
4	1,5	3,4,7	3,4,5,7	1,3,4,5,7
5	4,5	2,5,7	1,3,4,5	1,2,3,5,7
6	2,5	2,3,4	2,3,4,7	1,2,3,4,7

Table 4 - Classification performance of the training areas using TM band combinations 2,4,5 and 2,4,5 and 7.

	TM BAND COMBINATION	
	2,4,5	2,4,5,7
Average correct Classification	99.1%	99.1%
Average Omission error	0.2%	0.1%
Average Commission error	0.7%	0.8%
Upper band of the probability of error	9%	7%
Computer processing time	4min. 25sec.	4min. 30sec.

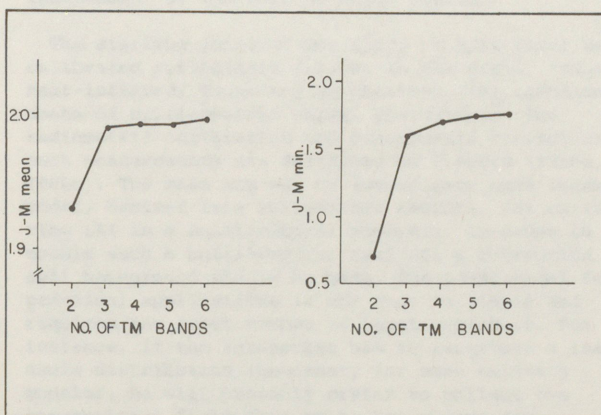


Fig. 1 - Separability of the best TM band combination selected by J-M distance.

as the best to discriminate soybeans, corn and sugarcane in the area.

- Separability of J-M distance indicated that the statistical structure for crop discrimination was three- or four-dimensional. Comparison of the classification matrices of the training areas using band combinations 2-4-5 and 2-4-5-7 showed similar results and a small difference in computer processing time. However, the smaller data storage volume of the three-band classification makes it the most appropriate for crop discrimination using digital analysis in this study area.

REFERENCES

- Anuta, P.E., Bartolucci L.A., Dean, M.E., Lazano, D.F., Malaret E., McGillem C.D., 1984 Landsat-4 MSS and Thematic Mapper data quality and information content analysis. IEEE Trans. on Geosci. and Remote Sens. GE-22(3): 222-235.
- Atkinson P., Cushnie J.L. and Townshend J.R.G. 1985. Improving Thematic Mapper land cover classification using filtered data. Int. J. Remote Sens. 6(6): 955-961.
- Salomonson, V.V., Smith P.L., Pink A.B., Webb, W.C., and Lynch T.J. 1980. An overview of progress in the design and implementation of Landsat D systems I.E.E.E. Trans. Geosci. Remote Sensing 18:137-146.
- Sheffield C., 1985. Selecting band combinations from multispectral data. Photogram. Eng. Remote Sens. 51(6): 681-687.
- Swain, P.M., King, R.C. 1973. Two effective feature selection criterion for multispectral remote sensing. IARS information note 402673 West Lafayette, Purdue University.
- Townshend, J.R.G., Gayler, J.R., Hardy, J.R., Jackson M.J., and Baker, J.R. 1983. Preliminary analysis of Landsat-4 Thematic Mapper products. Int. J. Remote Sens. 4 (4): 817-828.
- Townshend J.R.G. 1984 Agricultural land-cover discrimination using thematic mapper spectral bands. Int. J. Remote Sens. 5(4): 681-698.
- Young, T.Y., Calvert, T.W. 1974. Classification estimation and pattern recognition. New York, Elsevier.

Figure 1 shows the results of the discriminant analysis for the three crops. The discriminant function for soybeans is shown in the top panel, for corn in the middle panel, and for sugarcane in the bottom panel. The discriminant function for soybeans is $Y = 0.0001X_1 + 0.0002X_2 + 0.0003X_3 - 0.0004X_4 + 0.0005X_5 - 0.0006X_6 + 0.0007X_7 - 0.0008X_8 + 0.0009X_9 - 0.0010X_{10} + 0.0011X_{11} - 0.0012X_{12} + 0.0013X_{13} - 0.0014X_{14} + 0.0015X_{15} - 0.0016X_{16} + 0.0017X_{17} - 0.0018X_{18} + 0.0019X_{19} - 0.0020X_{20} + 0.0021X_{21} - 0.0022X_{22} + 0.0023X_{23} - 0.0024X_{24} + 0.0025X_{25} - 0.0026X_{26} + 0.0027X_{27} - 0.0028X_{28} + 0.0029X_{29} - 0.0030X_{30} + 0.0031X_{31} - 0.0032X_{32} + 0.0033X_{33} - 0.0034X_{34} + 0.0035X_{35} - 0.0036X_{36} + 0.0037X_{37} - 0.0038X_{38} + 0.0039X_{39} - 0.0040X_{40} + 0.0041X_{41} - 0.0042X_{42} + 0.0043X_{43} - 0.0044X_{44} + 0.0045X_{45} - 0.0046X_{46} + 0.0047X_{47} - 0.0048X_{48} + 0.0049X_{49} - 0.0050X_{50} + 0.0051X_{51} - 0.0052X_{52} + 0.0053X_{53} - 0.0054X_{54} + 0.0055X_{55} - 0.0056X_{56} + 0.0057X_{57} - 0.0058X_{58} + 0.0059X_{59} - 0.0060X_{60} + 0.0061X_{61} - 0.0062X_{62} + 0.0063X_{63} - 0.0064X_{64} + 0.0065X_{65} - 0.0066X_{66} + 0.0067X_{67} - 0.0068X_{68} + 0.0069X_{69} - 0.0070X_{70} + 0.0071X_{71} - 0.0072X_{72} + 0.0073X_{73} - 0.0074X_{74} + 0.0075X_{75} - 0.0076X_{76} + 0.0077X_{77} - 0.0078X_{78} + 0.0079X_{79} - 0.0080X_{80} + 0.0081X_{81} - 0.0082X_{82} + 0.0083X_{83} - 0.0084X_{84} + 0.0085X_{85} - 0.0086X_{86} + 0.0087X_{87} - 0.0088X_{88} + 0.0089X_{89} - 0.0090X_{90} + 0.0091X_{91} - 0.0092X_{92} + 0.0093X_{93} - 0.0094X_{94} + 0.0095X_{95} - 0.0096X_{96} + 0.0097X_{97} - 0.0098X_{98} + 0.0099X_{99} - 0.0100X_{100} + 0.0101X_{101} - 0.0102X_{102} + 0.0103X_{103} - 0.0104X_{104} + 0.0105X_{105} - 0.0106X_{106} + 0.0107X_{107} - 0.0108X_{108} + 0.0109X_{109} - 0.0110X_{110} + 0.0111X_{111} - 0.0112X_{112} + 0.0113X_{113} - 0.0114X_{114} + 0.0115X_{115} - 0.0116X_{116} + 0.0117X_{117} - 0.0118X_{118} + 0.0119X_{119} - 0.0120X_{120} + 0.0121X_{121} - 0.0122X_{122} + 0.0123X_{123} - 0.0124X_{124} + 0.0125X_{125} - 0.0126X_{126} + 0.0127X_{127} - 0.0128X_{128} + 0.0129X_{129} - 0.0130X_{130} + 0.0131X_{131} - 0.0132X_{132} + 0.0133X_{133} - 0.0134X_{134} + 0.0135X_{135} - 0.0136X_{136} + 0.0137X_{137} - 0.0138X_{138} + 0.0139X_{139} - 0.0140X_{140} + 0.0141X_{141} - 0.0142X_{142} + 0.0143X_{143} - 0.0144X_{144} + 0.0145X_{145} - 0.0146X_{146} + 0.0147X_{147} - 0.0148X_{148} + 0.0149X_{149} - 0.0150X_{150} + 0.0151X_{151} - 0.0152X_{152} + 0.0153X_{153} - 0.0154X_{154} + 0.0155X_{155} - 0.0156X_{156} + 0.0157X_{157} - 0.0158X_{158} + 0.0159X_{159} - 0.0160X_{160} + 0.0161X_{161} - 0.0162X_{162} + 0.0163X_{163} - 0.0164X_{164} + 0.0165X_{165} - 0.0166X_{166} + 0.0167X_{167} - 0.0168X_{168} + 0.0169X_{169} - 0.0170X_{170} + 0.0171X_{171} - 0.0172X_{172} + 0.0173X_{173} - 0.0174X_{174} + 0.0175X_{175} - 0.0176X_{176} + 0.0177X_{177} - 0.0178X_{178} + 0.0179X_{179} - 0.0180X_{180} + 0.0181X_{181} - 0.0182X_{182} + 0.0183X_{183} - 0.0184X_{184} + 0.0185X_{185} - 0.0186X_{186} + 0.0187X_{187} - 0.0188X_{188} + 0.0189X_{189} - 0.0190X_{190} + 0.0191X_{191} - 0.0192X_{192} + 0.0193X_{193} - 0.0194X_{194} + 0.0195X_{195} - 0.0196X_{196} + 0.0197X_{197} - 0.0198X_{198} + 0.0199X_{199} - 0.0200X_{200} + 0.0201X_{201} - 0.0202X_{202} + 0.0203X_{203} - 0.0204X_{204} + 0.0205X_{205} - 0.0206X_{206} + 0.0207X_{207} - 0.0208X_{208} + 0.0209X_{209} - 0.0210X_{210} + 0.0211X_{211} - 0.0212X_{212} + 0.0213X_{213} - 0.0214X_{214} + 0.0215X_{215} - 0.0216X_{216} + 0.0217X_{217} - 0.0218X_{218} + 0.0219X_{219} - 0.0220X_{220} + 0.0221X_{221} - 0.0222X_{222} + 0.0223X_{223} - 0.0224X_{224} + 0.0225X_{225} - 0.0226X_{226} + 0.0227X_{227} - 0.0228X_{228} + 0.0229X_{229} - 0.0230X_{230} + 0.0231X_{231} - 0.0232X_{232} + 0.0233X_{233} - 0.0234X_{234} + 0.0235X_{235} - 0.0236X_{236} + 0.0237X_{237} - 0.0238X_{238} + 0.0239X_{239} - 0.0240X_{240} + 0.0241X_{241} - 0.0242X_{242} + 0.0243X_{243} - 0.0244X_{244} + 0.0245X_{245} - 0.0246X_{246} + 0.0247X_{247} - 0.0248X_{248} + 0.0249X_{249} - 0.0250X_{250} + 0.0251X_{251} - 0.0252X_{252} + 0.0253X_{253} - 0.0254X_{254} + 0.0255X_{255} - 0.0256X_{256} + 0.0257X_{257} - 0.0258X_{258} + 0.0259X_{259} - 0.0260X_{260} + 0.0261X_{261} - 0.0262X_{262} + 0.0263X_{263} - 0.0264X_{264} + 0.0265X_{265} - 0.0266X_{266} + 0.0267X_{267} - 0.0268X_{268} + 0.0269X_{269} - 0.0270X_{270} + 0.0271X_{271} - 0.0272X_{272} + 0.0273X_{273} - 0.0274X_{274} + 0.0275X_{275} - 0.0276X_{276} + 0.0277X_{277} - 0.0278X_{278} + 0.0279X_{279} - 0.0280X_{280} + 0.0281X_{281} - 0.0282X_{282} + 0.0283X_{283} - 0.0284X_{284} + 0.0285X_{285} - 0.0286X_{286} + 0.0287X_{287} - 0.0288X_{288} + 0.0289X_{289} - 0.0290X_{290} + 0.0291X_{291} - 0.0292X_{292} + 0.0293X_{293} - 0.0294X_{294} + 0.0295X_{295} - 0.0296X_{296} + 0.0297X_{297} - 0.0298X_{298} + 0.0299X_{299} - 0.0300X_{300} + 0.0301X_{301} - 0.0302X_{302} + 0.0303X_{303} - 0.0304X_{304} + 0.0305X_{305} - 0.0306X_{306} + 0.0307X_{307} - 0.0308X_{308} + 0.0309X_{309} - 0.0310X_{310} + 0.0311X_{311} - 0.0312X_{312} + 0.0313X_{313} - 0.0314X_{314} + 0.0315X_{315} - 0.0316X_{316} + 0.0317X_{317} - 0.0318X_{318} + 0.0319X_{319} - 0.0320X_{320} + 0.0321X_{321} - 0.0322X_{322} + 0.0323X_{323} - 0.0324X_{324} + 0.0325X_{325} - 0.0326X_{326} + 0.0327X_{327} - 0.0328X_{328} + 0.0329X_{329} - 0.0330X_{330} + 0.0331X_{331} - 0.0332X_{332} + 0.0333X_{333} - 0.0334X_{334} + 0.0335X_{335} - 0.0336X_{336} + 0.0337X_{337} - 0.0338X_{338} + 0.0339X_{339} - 0.0340X_{340} + 0.0341X_{341} - 0.0342X_{342} + 0.0343X_{343} - 0.0344X_{344} + 0.0345X_{345} - 0.0346X_{346} + 0.0347X_{347} - 0.0348X_{348} + 0.0349X_{349} - 0.0350X_{350} + 0.0351X_{351} - 0.0352X_{352} + 0.0353X_{353} - 0.0354X_{354} + 0.0355X_{355} - 0.0356X_{356} + 0.0357X_{357} - 0.0358X_{358} + 0.0359X_{359} - 0.0360X_{360} + 0.0361X_{361} - 0.0362X_{362} + 0.0363X_{363} - 0.0364X_{364} + 0.0365X_{365} - 0.0366X_{366} + 0.0367X_{367} - 0.0368X_{368} + 0.0369X_{369} - 0.0370X_{370} + 0.0371X_{371} - 0.0372X_{372} + 0.0373X_{373} - 0.0374X_{374} + 0.0375X_{375} - 0.0376X_{376} + 0.0377X_{377} - 0.0378X_{378} + 0.0379X_{379} - 0.0380X_{380} + 0.0381X_{381} - 0.0382X_{382} + 0.0383X_{383} - 0.0384X_{384} + 0.0385X_{385} - 0.0386X_{386} + 0.0387X_{387} - 0.0388X_{388} + 0.0389X_{389} - 0.0390X_{390} + 0.0391X_{391} - 0.0392X_{392} + 0.0393X_{393} - 0.0394X_{394} + 0.0395X_{395} - 0.0396X_{396} + 0.0397X_{397} - 0.0398X_{398} + 0.0399X_{399} - 0.0400X_{400} + 0.0401X_{401} - 0.0402X_{402} + 0.0403X_{403} - 0.0404X_{404} + 0.0405X_{405} - 0.0406X_{406} + 0.0407X_{407} - 0.0408X_{408} + 0.0409X_{409} - 0.0410X_{410} + 0.0411X_{411} - 0.0412X_{412} + 0.0413X_{413} - 0.0414X_{414} + 0.0415X_{415} - 0.0416X_{416} + 0.0417X_{417} - 0.0418X_{418} + 0.0419X_{419} - 0.0420X_{420} + 0.0421X_{421} - 0.0422X_{422} + 0.0423X_{423} - 0.0424X_{424} + 0.0425X_{425} - 0.0426X_{426} + 0.0427X_{427} - 0.0428X_{428} + 0.0429X_{429} - 0.0430X_{430} + 0.0431X_{431} - 0.0432X_{432} + 0.0433X_{433} - 0.0434X_{434} + 0.0435X_{435} - 0.0436X_{436} + 0.0437X_{437} - 0.0438X_{438} + 0.0439X_{439} - 0.0440X_{440} + 0.0441X_{441} - 0.0442X_{442} + 0.0443X_{443} - 0.0444X_{444} + 0.0445X_{445} - 0.0446X_{446} + 0.0447X_{447} - 0.0448X_{448} + 0.0449X_{449} - 0.0450X_{450} + 0.0451X_{451} - 0.0452X_{452} + 0.0453X_{453} - 0.0454X_{454} + 0.0455X_{455} - 0.0456X_{456} + 0.0457X_{457} - 0.0458X_{458} + 0.0459X_{459} - 0.0460X_{460} + 0.0461X_{461} - 0.0462X_{462} + 0.0463X_{463} - 0.0464X_{464} + 0.0465X_{465} - 0.0466X_{466} + 0.0467X_{467} - 0.0468X_{468} + 0.0469X_{469} - 0.0470X_{470} + 0.0471X_{471} - 0.0472X_{472} + 0.0473X_{473} - 0.0474X_{474} + 0.0475X_{475} - 0.0476X_{476} + 0.0477X_{477} - 0.0478X_{478} + 0.0479X_{479} - 0.0480X_{480} + 0.0481X_{481} - 0.0482X_{482} + 0.0483X_{483} - 0.0484X_{484} + 0.0485X_{485} - 0.0486X_{486} + 0.0487X_{487} - 0.0488X_{488} + 0.0489X_{489} - 0.0490X_{490} + 0.0491X_{491} - 0.0492X_{492} + 0.0493X_{493} - 0.0494X_{494} + 0.0495X_{495} - 0.0496X_{496} + 0.0497X_{497} - 0.0498X_{498} + 0.0499X_{499} - 0.0500X_{500} + 0.0501X_{501} - 0.0502X_{502} + 0.0503X_{503} - 0.0504X_{504} + 0.0505X_{505} - 0.0506X_{506} + 0.0507X_{507} - 0.0508X_{508} + 0.0509X_{509} - 0.0510X_{510} + 0.0511X_{511} - 0.0512X_{512} + 0.0513X_{513} - 0.0514X_{514} + 0.0515X_{515} - 0.0516X_{516} + 0.0517X_{517} - 0.0518X_{518} + 0.0519X_{519} - 0.0520X_{520} + 0.0521X_{521} - 0.0522X_{522} + 0.0523X_{523} - 0.0524X_{524} + 0.0525X_{525} - 0.0526X_{526} + 0.0527X_{527} - 0.0528X_{528} + 0.0529X_{529} - 0.0530X_{530} + 0.0531X_{531} - 0.0532X_{532} + 0.0533X_{533} - 0.0534X_{534} + 0.0535X_{535} - 0.0536X_{536} + 0.0537X_{537} - 0.0538X_{538} + 0.0539X_{539} - 0.0540X_{540} + 0.0541X_{541} - 0.0542X_{542} + 0.0543X_{543} - 0.0544X_{544} + 0.0545X_{545} - 0.0546X_{546} + 0.0547X_{547} - 0.0548X_{548} + 0.0549X_{549} - 0.0550X_{550} + 0.0551X_{551} - 0.0552X_{552} + 0.0553X_{553} - 0.0554X_{554} + 0.0555X_{555} - 0.0556X_{556} + 0.0557X_{557} - 0.0558X_{558} + 0.0559X_{559} - 0.0560X_{560} + 0.0561X_{561} - 0.0562X_{562} + 0.0563X_{563} - 0.0564X_{564} + 0.0565X_{565} - 0.0566X_{566} + 0.0567X_{567} - 0.0568X_{568} + 0.0569X_{569} - 0.0570X_{570} + 0.0571X_{571} - 0.0572X_{572} + 0.0573X_{573} - 0.0574X_{574} + 0.0575X_{575} - 0.0576X_{576} + 0.0577X_{577} - 0.0578X_{578} + 0.0579X_{579} - 0.0580X_{580} + 0.0581X_{581} - 0.0582X_{582} + 0.0583X_{583} - 0.0584X_{584} + 0.0585X_{585} - 0.0586X_{586} + 0.0587X_{587} - 0.0588X_{588} + 0.0589X_{589} - 0.0590X_{590} + 0.0591X_{591} - 0.0592X_{592} + 0.0593X_{593} - 0.0594X_{594} + 0.0595X_{595} - 0.0596X_{596} + 0.0597X_{597} - 0.0598X_{598} + 0.0599X_{599} - 0.0600X_{600} + 0.0601X_{601} - 0.0602X_{602} + 0.0603X_{603} - 0.0604X_{604} + 0.0605X_{605} - 0.0606X_{606} + 0.0607X_{607} - 0.0608X_{608} + 0.0609X_{609} - 0.0610X_{610} + 0.0611X_{611} - 0.0612X_{612} + 0.0613X_{613} - 0.0614X_{614} + 0.0615X_{615} - 0.0616X_{616} + 0.0617X_{617} - 0.0618X_{618} + 0.0619X_{619} - 0.0620X_{620} + 0.0621X_{621} - 0.0622X_{622} + 0.0623X_{623} - 0.0624X_{624} + 0.0625X_{625} - 0.0626X_{626} + 0.0627X_{627} - 0.0628X_{628} + 0.0629X_{629} - 0.0630X_{630} + 0.0631X_{631} - 0.0632X_{632} + 0.0633X_{633} - 0.0634X_{634} + 0.0635X_{635} - 0.0636X_{636} + 0.0637X_{637} - 0.0638X_{638} + 0.0639X_{639} - 0.0640X_{640} + 0.0641X_{641} - 0.0642X_{642} + 0.0643X_{643} - 0.0644X_{644} + 0.0645X_{645} - 0.0646X_{646} + 0.0647X_{647} - 0.0648X_{648} + 0.0649X_{649} - 0.0650X_{650} + 0.0651X_{651} - 0.0652X_{652} + 0.0653X_{653} - 0.0654X_{654} + 0.0655X_{655} - 0.0656X_{656} + 0.0657X_{657} - 0.0658X_{658} + 0.0659X_{659} - 0.0660X_{660} + 0.0661X_{661} - 0.0662X_{662} + 0.0663X_{663} - 0.0664X_{664} + 0.0665X_{665} - 0.0666X_{666} + 0.0667X_{667} - 0.0668X_{668} + 0.0669X_{669} - 0.0670X_{670} + 0.0671X_{671} - 0.0672X_{672} + 0.0673X_{673} - 0.0674X_{674} + 0.0675X_{675} - 0.0676X_{676} + 0.0677X_{677} - 0.0678X_{678} + 0.0679X_{679} - 0.0680X_{680} + 0.0681X_{681} - 0.0682X_{682} + 0.0683X_{683} - 0.0684X_{684} + 0.0685X_{685} - 0.0686X_{686} + 0.0687X_{687} - 0.0688X_{688} + 0.0689X_{689} - 0.0690X_{690} + 0.0691X_{691} - 0.0692X_{692} + 0.0693X_{693} - 0.0694X_{694} + 0.0695X_{695} - 0.0696X_{696} + 0.0697X_{697} - 0.0698X_{698} + 0.0699X_{699} - 0.0700X_{700} + 0.0701X_{701} - 0.0702X_{702} + 0.0703X_{703} - 0.0704X_{704} + 0.0705X_{705} - 0.0706X_{706} + 0.0707X_{707} - 0.0708X_{708} + 0.0709X_{709} - 0.0710X_{710} + 0.0711X_{711} - 0.0712X_{712} + 0.0713X_{713} - 0.0714X_{714} + 0.0715X_{715} - 0.0716X_{716} + 0.0717X_{717} - 0.0718X_{718} + 0.0719X_{719} - 0.0720X_{720} + 0.0721X_{721} - 0.0722X_{722} + 0.0723X_{723} - 0.0724X_{724} + 0.0725X_{725} - 0.0726X_{726} + 0.0727X_{727} - 0.0728X_{728} + 0.0729X_{729} - 0.0730X_{730} + 0.0731X_{731} - 0.0732X_{732} + 0.0733X_{733} - 0.0734X_{734} + 0.0735X_{735} - 0.0736X_{736} + 0.0737X_{737} - 0.0738X_{738} + 0.0739X_{739} - 0.0740X_{740} + 0.0741X_{741} - 0.0742X_{742} + 0.0743X_{743} - 0.0744X_{744} + 0.0745X_{745} - 0.0746X_{746} + 0.0747X_{747} - 0.0748X_{748} + 0.0749X_{749} - 0.0750X_{750} + 0.0751X_{751} - 0.0752X_{752} + 0.0753X_{753} - 0.0754X_{754} + 0.0755X_{755} - 0.0756X_{756} + 0.0757X_{757} - 0.0758X_{758} + 0.0759X_{759} - 0.0760X_{760} + 0.0761X_{761} - 0.0762X_{762} + 0.0763X_{763} - 0.0764X_{764} + 0.0765X_{765} - 0.0766X_{766} + 0.0767X_{767} - 0.0768X_{768} + 0.0769X_{769} - 0.0770X_{770} + 0.0771X_{771} - 0.0772X_{772} + 0.0773X_{773} - 0.0774X_{774} + 0.0775X_{775} - 0.0776X_{776} + 0.0777X_{777} - 0.0778X_{778} + 0.0779X_{779} - 0.0780X_{780} + 0.0781X_{781} - 0.0782X_{782} + 0.0783X_{783} - 0.0784X_{784} + 0.0785X_{785} - 0.0786X_{786} + 0.0787X_{787} - 0.0788X_{788} + 0.0789X_{789} - 0.0790X_{790} + 0.0791X_{791} - 0.0792X_{792} + 0.0793X_{793} - 0.0794X_{794} + 0.0795X_{795} - 0.0796X_{796} + 0.0797X_{797} - 0.0798X_{798} + 0.0799X_{799} - 0.0800X_{800} + 0.0801X_{801} - 0.0802X_{802} + 0.0803X_{803} - 0.0804X_{804} + 0.0805X_{805} - 0.0806X_{806} + 0.0807X_{807} - 0.0808X_{808} + 0.0809X_{809} - 0.0810X_{810} + 0.0811X_{811} - 0.0812X_{812} + 0.0813X_{813} - 0.0814X_{814} + 0.0815X_{815} - 0.0816X_{816} + 0.0817X_{817} - 0.0818X_{818} + 0.0819X_{819} - 0.0820X_{820} + 0.0821X_{821} - 0.0822X_{822} + 0.0823X_{823} - 0.0824X_{824} + 0.0825X_{825} - 0.0826X_{826} + 0.0827X_{827} - 0.0828X_{828} + 0.0829X_{829} - 0.0830X_{830} + 0.0831X_{831} - 0.0832X_{832} + 0.0833X_{833} - 0.0834X_{834} + 0.0835X_{8$